Metabolic Engineering 13 (2011) 345–352

Contents lists available at ScienceDirect

Metabolic Engineering

journal homepage: www.elsevier.com/locate/ymben

Engineered ketol-acid reductoisomerase and alcohol dehydrogenase enable anaerobic 2-methylpropan-1-ol production at theoretical yield in *Escherichia coli*

Sabine Bastian [a], Xiang Liu [a,1], Joseph T. Meyerowitz [a], Christopher D. Snow [a], Mike M.Y. Chen [a], Frances H. Arnold [a,*]

[a] Division of Chemistry and Chemical Engineering, California Institute of Technology, Mail code 210-41, Pasadena, CA 91125, USA

ARTICLE INFO

Keywords:
Metabolic engineering
Cofactor imbalance
Isobutanol
Ketol-acid reductoisomerase
Biofuels

ABSTRACT

2-methylpropan-1-ol (isobutanol) is a leading candidate biofuel for the replacement or supplementation of current fossil fuels. Recent work has demonstrated glucose to isobutanol conversion through a modified amino acid pathway in a recombinant organism. Although anaerobic conditions are required for an economically competitive process, only aerobic isobutanol production has been feasible due to an imbalance in cofactor utilization. Two of the pathway enzymes, ketol-acid reductoisomerase and alcohol dehydrogenase, require nicotinamide dinucleotide phosphate (NADPH); glycolysis, however, produces only nicotinamide dinucleotide (NADH). Here, we compare two solutions to this imbalance problem: (1) over-expression of pyridine nucleotide transhydrogenase PntAB and (2) construction of an NADH-dependent pathway, using engineered enzymes. We demonstrate that an NADH-dependent pathway enables anaerobic isobutanol production at 100% theoretical yield and at higher titer and productivity than both the NADPH-dependent pathway and transhydrogenase over-expressing strain. Our results show how engineering cofactor dependence can overcome a critical obstacle to next-generation biofuel commercialization.

1. Introduction

Recent advances in biotechnology have made it possible to convert sugars into a wide array of renewable chemicals (Liu and Khosla, 2010; Rude and Schirmer, 2009; Shen and Liao, 2008; Yan and Liao, 2009). Of all these possibilities, isobutanol, an excellent gasoline blend stock and precursor to C4 petrochemical building blocks, is especially promising because of its potential for high-yield production and compatibility with an existing fuel infrastructure (Rude and Schirmer, 2009). Isobutanol is an energy-dense, low-vapor-pressure, high-octane hydrocarbon that burns in a combustion engine like conventional gasoline without adversely affecting the performance (Bruno et al., 2010; Szwaja and Naber, 2010). Isobutanol is also readily converted to butenes that can be used directly to produce hydrocarbon-based fuels, commodity chemicals, and materials (Connor and Liao, 2009; Taylor et al., 2010). For these renewables to be cost-competitive with conventional fuel and butenes, fermentation of sugars to isobutanol must be as efficient as bioethanol production, which reaches commercial viability through anaerobic, high-productivity, high-titer, and high-yield fermentation performance in low capital cost production facilities.

Although the Ehrlich pathway (Ehrlich, 1907), the catabolic process that converts amino acid precursors to fusel alcohols, has long been known in yeast (Hazelwood et al., 2008), industrially relevant production of higher alcohols in native microorganisms has not been demonstrated (Alper and Stephanopoulos, 2009). Isobutanol fermentation has become feasible via an implementation of a synthetic Ehrlich pathway in *Escherichia coli*, where 2-keto-isovalerate serves as precursor for isobutanol (Atsumi et al., 2008b) (Fig. 1). The use of engineered strains with deletions in pathways competing for carbon and cofactors (Atsumi et al., 2008a) has enabled isobutanol titers of >20 g/L to be reached aerobically or micro-aerobically (Atsumi et al., 2008b; Atsumi et al., 2010). However, anaerobic conditions are preferred for large-scale production due to lower operating costs and higher theoretical yield. We hypothesized that the limited isobutanol production observed under anaerobic conditions is caused by a cofactor imbalance in the engineered pathway. Two of the five pathway enzymes are nicotinamide adenine dinucleotide phosphate (NADPH)-dependent: (1) ketol-acid reductoisomerase

* Corresponding author. Fax: +1 626 568 8743.
E-mail address:
frances@cheme.caltech.edu (F.H. Arnold).
[1] Permanent address: Laboratory of Biocatalysis and Bioprocessing, State Key Laboratory of Bioreactor Engineering, East China University of Science and Technology, 130 Meilong Road, Shanghai 200237, PR China.

1096-7176/$ - see front matter © 2011 Elsevier Inc. All rights reserved.
doi:10.1016/j.ymben.2011.02.004

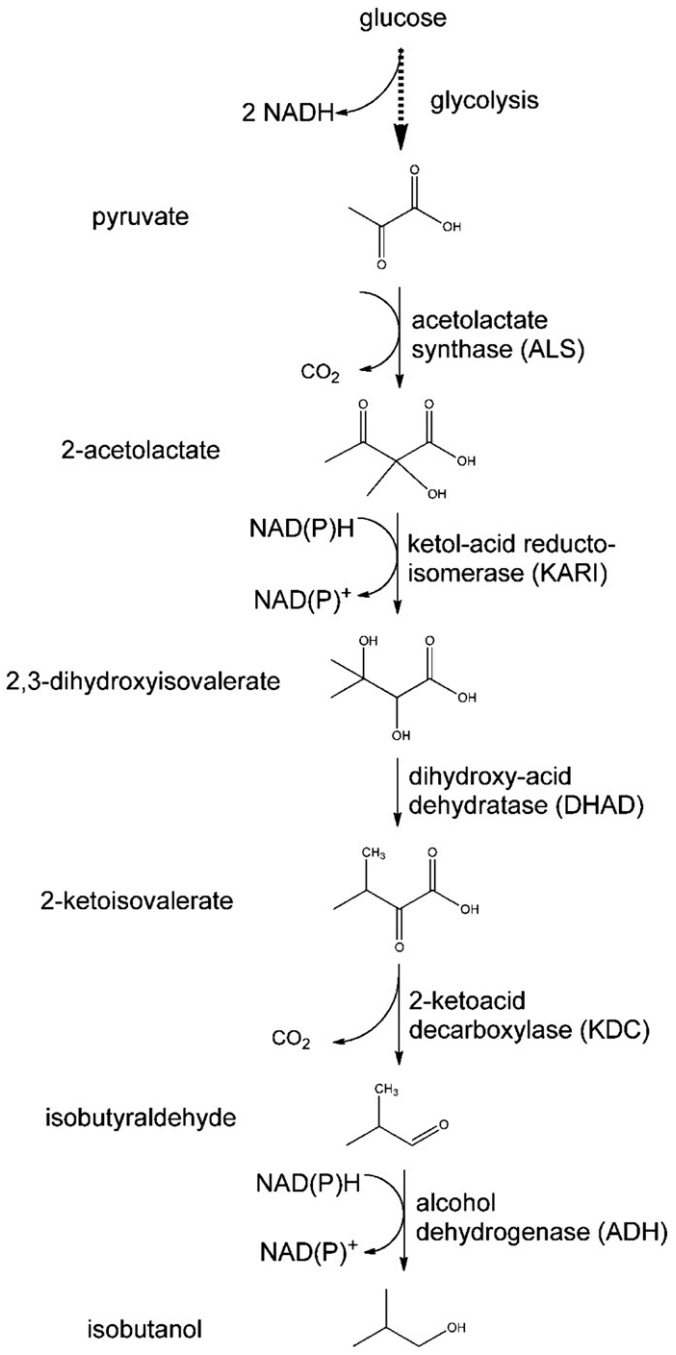

Fig. 1. Engineered pathway for isobutanol production (Atsumi et al., 2010). Acetolactate synthase (ALS), ketol-acid reductoisomerase (KARI), dihydroxy-acid dehydratase (DHAD), 2-ketoacid decarboxylase (KDC), and alcohol dehydrogenase (ADH).

(KARI, IlvC from *E. coli*; EC 1.1.1.86) catalyzes the two-step reaction from *S*-2-acetolactate (*S*-2-AL) to 2,3-dihydroxy-isovalerate (DHIV), involving a Mg^{2+}-dependent alkyl migration followed by ketone reduction (Chunduru et al., 1989), and (2) alcohol dehydrogenase (ADH, YqhD from *E. coli*; EC 1.1.1.2) reduces isobutyraldehyde to isobutanol (Atsumi et al., 2010) (Fig. 1). Thus, the conversion of glucose to isobutanol requires two equivalents of NADPH. Under anaerobic conditions, however, the only available reducing equivalent is nicotinamide adenine dinucleotide (NADH), produced through glycolysis. The cells cannot resolve this cofactor imbalance via the pentose phosphate pathway (PPP) or the tricarboxylic acid (TCA) cycle, because these are functional only in the presence of oxygen. NADPH-limited reactions have been previously noted in commercially relevant systems such as the production of xylitol (Chin et al., 2009) and the production of n-butanol (Steen et al., 2008).

One possible solution to a cofactor imbalance is to overexpress a transhydrogenase, such as *E. coli* PntAB (Weckbecker and Hummel, 2004), which catalyzes the reversible transfer of a hydride ion between NADH and $NADP^+$. This transfer is coupled to the proton motive force and uses one proton per hydride (Clarke and Bragg, 1985; Sauer et al., 2004). This energy requirement and the metabolic load associated with expression of the transhydrogenase are two drawbacks to this approach (Chin et al., 2009). As an alternative solution, Liao (Atsumi et al., 2010) and we propose to replace the NADPH-dependent enzymes of the pathway with NADH-utilizing homologs. Substituting the ADH with an NADH-dependent homolog is feasible due to the abundance of known NADH-dependent ADHs (Jornvall et al., 1987). For example, AdhA from *Lactococcus lactis* has been shown previously to be compatible with the isobutanol pathway (Atsumi et al., 2010). However, an NADH-dependent enzyme, catalyzing the conversion of *S*-2-AL to DHIV, has yet to be reported.

We therefore aimed to switch the cofactor dependence of the native *E. coli* IlvC from NADPH to NADH. Although there are literature examples of engineered changes in cofactor preference, reports of specificity reversals are rare (Ehsani et al., 2009). Examples in which the engineered enzyme is placed back into a pathway have shown only limited success in resolving the cofactor imbalance (Matsushika et al., 2008a, 2008b; Petschacher and Nidetzky, 2008). In this study, we describe the engineering of an NADH-dependent IlvC by directed evolution, using iterative, targeted mutagenesis. Upon recombining beneficial mutations, we found two variants with acetolactate (2-AL) reducing activity in the presence of NADH that is similar to the wild-type enzyme with NADPH. Utilizing the best IlvC variant and an engineered *L. lactis* AdhA variant in the isobutanol pathway improved the yield to 100% of the theoretical limit under anaerobic conditions. We demonstrate that (a) reversal of the cofactor preference of IlvC can be achieved, and (b) by engineering the cofactor dependence of the isobutanol metabolic pathway, the NADH-dependent pathway outperforms over-expression of a transhydrogenase for resolving the cofactor imbalance and the engineered pathway achieves the highest possible yield.

2. Materials and methods

2.1. General

Strain 1993 and plasmids pGV1662, pGV1777, pGV1925, pGV1947, pGV1711, and pGV1705 are to be found in Table A, Appendix A. Biological media were purchased from Research Products International (Mt. Prospect, IL, USA), NAD(P)H from Codexis, Inc. (Redwood City, CA, USA), oligonucleotides from Integrated DNA Technologies (San Diego, CA, USA), DNA polymerases, restriction enzymes, and T4 ligase from New England Biolabs (Ipswich, MA, USA), and ethyl 2-acetoxy-2-methylacetoacetate (EAMAA) from Sigma (St. Louis, MO, USA). (*R/S*)-2-acetolactate (2-AL) was prepared as described previously (Krampitz, 1957), using EAMAA as starting material. DNA sequencing was performed by Laragen (Los Angeles, CA, USA). Standard molecular biology methods were taken from Maniatis et al. (Sambrook et al., 1989).

2.2. Structure alignment

Mutation sites were selected following an inspection of the cofactor-binding site. To assess cofactor side-chain interactions, we used PyMOL Molecular Graphics System (Version 1.3,

Schrödinger, LLC) to prepare an alignment of the X-ray crystal structures of *E. coli* IlvC (1YRL (Tyagi et al., 2005)) and spinach KARI (1YVE (Biou et al., 1997)).

2.3. Cloning and library construction

Primers, plasmids, and strains are listed in Tables A and B, Appendix A. The gene encoding *E. coli* IlvC was cloned into pET22(b)+(EMD Chemicals Group, Darmstadt, Germany) for expression in *E. coli* BL21(DE3) using *Nde*I and *Xho*I restriction sites (Lucigen Corporation, Middleton, WI, USA). The gene encoding *L. lactis* AdhA was cloned into pGV1662 for expression in *S. cerevisiae* CEN.PK2 (EUROSCARF, Frankfurt, Germany), using *Not*I and *Sal*I restriction sites. All primers are listed in Table B, Appendix A. Error-prone PCR was performed according to a published protocol (Bloom et al., 2006). Point mutations, site-saturation mutagenesis, and recombination libraries were made by splicing by overlap extension PCR (Kunkel et al., 1987). For recombination libraries, primers with degenerate codons were used when possible. The IlvC recombination library was constructed using SOE PCR to introduce beneficial mutations identified at the five targeted sites, while allowing for wild-type sequence as well. The first fragments were generated with degenerate primers R68A71recombfor and R68A71recombrev. The clean assembly product served as template for a second round of SOE PCR introducing mutations at positions 76 and 78 with a mixture of equimolar concentrations of primers. The resulting assembly product served as template to complete the recombination library with the introduction of mutations at amino acid position 110, using an equimolar mix of the mutagenic primers for position 110. We cloned the complete assembly product into pET22b(+) using restriction sites *Nde*I and *Xho*I and transformed electro-competent BL21(D3) cells with the ligation mix. The AdhA recombination library was constructed by SOE PCR introducing beneficial mutations found in the error-prone library, while allowing for wild-type sequence at all targeted sites. After successful assembly PCR, homologous recombination, as described previously (Chao et al., 2006), was used to create the yeast libraries using the recombination PCR product as insert and pGV1662 as backbone.

2.4. Heterologous protein expression

IlvC wild type and variants were expressed in Luria–Bertani broth supplemented with ampicillin. The 100-mL expression cultures with the purpose of purification were grown at 250 rpm and 37 °C and were inoculated by overnight cultures to an optical density (OD_{600}) of 0.1. After reaching an OD_{600} of 1, isopropyl β-D-1-thiogalactopyranoside (IPTG) was added to a 0.5 mM final concentration for induction. The cultures were then continued for 24 h at 250 rpm and 25 °C. Cells were harvested by centrifugation. High throughput *E. coli* expression cultures (600 μL LB_{amp} in 96-well deep well plates) were inoculated with 75 μL of high throughput overnight cultures, and then grown for 4 h at 37 °C and 210 rpm in a humidified plate shaker (Kuhner, Switzerland). One hour before induction with IPTG at a final concentration of 0.5 mM, the temperature of the incubator was reduced to 25 °C. After induction, growth and expression continued for 24 h at 25 °C and 210 rpm. The cells were harvested by centrifugation and stored at −20 °C. $AdhA^{his6}$ and variants were expressed in SC-URA (6.7 g/L Yeast nitrogen base, 10 g/L casamino acids, 20 g/L glucose, 0.018 g/L adenine hemisulfate, and 0.076 g/L tryptophan) inoculated with 1/100 (for 96-well plates: 1:12 dilution) of an overnight culture. After growth at 30 °C and 250 rpm for 24 h, cells were pelleted by centrifugation and stored at −20 °C. Expression cultures for purification contained 100 mL of medium; high throughput cultures were grown in 600 μL SC-URA.

2.5. Protein purification

$IlvC^{his6}$, $AdhA^{his6}$, and their variants were purified by immobilized metal affinity chromatography (IMAC) over 1 mL Histrap High Performance (HP) columns precharged with nickel (GE Healthcare, Waukesha, WI, USA), using an AKTA FPLC system (GE Healthcare, Waukesha, WI, USA). All purification steps were performed at 4 °C. *E. coli* and yeast cell pellets were resuspended at a ratio of 0.25 g wet weight/mL in buffer A, consisting of 20 mM Tris pH 7.4, 20 mM imidazole, 100 mM NaCl, and 10 mM $MgCl_2$. The resuspended *E. coli* cells were lysed by sonication for 1 min with a 50% duty cycle (Misonix Inc., Farmingdale, NY, USA); the yeast cells were destroyed by bead beating for six 1-min cycles with a frequency of $30\ s^{-1}$ with 1 min of cooling on ice in between cycles (Retsch Inc., Newtown, PA, USA). The disrupted *E. coli* and yeast cells were then pelleted at 11,000*g* and 4 °C for 15 min. The purification method consisted of a 4-column volume equilibration step with buffer A followed by the injection of the crude extract and a washout unbound sample step with buffer A for two column volumes. The proteins were eluted with a linear gradient from buffer A to 100% buffer B (20 mM Tris pH 7.4, 300 mM imidazole, 100 mM NaCl, and 10 mM $MgCl_2$) over 10 column volumes. $IlvC^{his6}$, $AdhA^{his6}$, and variants eluted at 40% buffer B and were stored as is at 4 °C.

2.6. Kinetic assays and high-throughput screening

For the high-throughput assays, *E. coli* cells were lysed with 250 mM potassium phosphate pH 7, 750 mg/L lysozyme, and 10 mg/L DNaseI, and yeast cells were lysed with Y-Per (Pierce Biotechnology Inc., Rockford, IL, USA). IlvC and ADH activities were then assayed by monitoring NAD(P)H consumption at 340 nm in a plate reader (TECAN Group Ltd., Switzerland). The IlvC assay buffer contained 250 mM potassium phosphate pH 7, 1 mM DTT, 200 μM NAD(P)H, 10 mM 2-AL, and 10 mM $MgCl_2$. The ADH assay buffer contained 100 mM Tris, pH 7, 1 mM DTT, 10 mM isobutyraldehyde, and 200 μM NADH.

2.7. Plasmid and strain construction for fermentation, anaerobic shift fermentations, and analytics

For all constructs, *Eco*RI and *Not*I restriction sites flanked the *adh* genes (no his-tag), and *Not*I and *Avr*II restriction sites flanked the *ilvC* genes (with the his-tag). Strain 1993 was constructed by integrating PLlacO1::Ll_kivd1::Ec_ilvD_coEc::FRT into the *ilvC* locus of JCL260 (Atsumi et al., 2008a) using SOE (Horton et al., 1989), gene integration (Datsenko and Wanner, 2000), and P1 transduction. Next, PLlacO1::Bs_alsS1::FRT was integrated into the *pta* locus to yield 1993, and PLlacO1::pntAB::FRT was integrated in the *sthA* locus of 1993 to yield 1993mod as described above. Fermentations were performed in biological triplicates using M9 media (Miller, 1992) supplemented with 8.5% glucose, 10 g/L yeast extract, and trace metals (1000x stock: 0.286 g H_3BO_3, 0.18 g $MnCl_2 \cdot 4H_2O$, 0.022 g $ZnSO_4 \cdot 7H_2O$, 0.039 g $Na_2MoO_4 \cdot 2H_2O$, 0.0079 g $CuSO_4 \cdot 5H_2O$, and 0.0049 g $CoCl_2 \cdot 6H_2O$ in 100 mL water). Fermentation cultures (20 mL) were inoculated by overnight cultures to an OD_{600} of 0.1. Cells were incubated at 37 °C and 250 rpm to an OD_{600} of 0.8–1.0 followed by IPTG induction at 1 mM final concentration. The flasks were then incubated at 30 °C and 250 rpm to an OD_{600} of 4.0–6.0 before shifting to anaerobic conditions by flushing with oxygen-free atmosphere in an airlock (Coy Laboratory Products, Grass Lake,

MI, USA). The cultures were then incubated without shaking at 30 °C in an anaerobic chamber and were swirled twice a day. Samples were taken at the time of the anaerobic shift and 24 h after induction. Gas chromatography analysis for determination of the isobutanol concentration was performed with a ZB-FFAP column (Phenomenex, 30 m length, 0.32 mm ID, and 0.25 μM film thickness) and a flame ionization detector. The temperature program was: injector 230 °C, detector 300 °C, 100 °C oven for 1 min, 70 °C/min gradient to 245 °C, and hold for 2.5 min. High performance liquid chromatography analysis of glucose concentrations was performed with two Restek RFQ 100×7.8 mm columns in series using a UV (210 nm, Agilent Technologies Inc., Santa Clara, CA, USA) and a refractive index detector (Agilent Technologies Inc., Santa Clara, CA, USA). The column temperature was 60 °C, and the method was isocratic with 0.018 N H_2SO_4 in Milli-Q water with a 1.1 mL/min flow.

3. Results

3.1. Engineering of an NADH-dependent E. coli IlvC

An IlvC variant engineered for NADH preference was reported by Rane and Calvo (Rane and Calvo, 1997). We constructed that variant (R68D:K69L:K75V:R76D) and reproduced the reported NADH/NADPH activity (in U/mg) ratio of 2.5, which is 31-fold higher than that for wild-type IlvC. However, the purified variant exhibited decreased specific activity for 2-AL reduction with both NADPH and NADH (5- and 2-folds, respectively) and was unsuitable for anaerobic isobutanol fermentations, since the strain produced <1 g/L isobutanol after 24 h (data not shown). Thus, the gene coding for the NADPH-dependent wild-type *E. coli* IlvC was used as the starting point to engineer a highly active cofactor-switched IlvC variant that will support anaerobic fermentation. The structure of IlvC has been reported without the cofactor (Tyagi et al., 2005). Therefore, a structural alignment of IlvC with its spinach homolog co-crystallized with NADPH (Biou et al., 1997) was used to identify amino acid residues R68, A71, R76, S78, and Q110 as targets for mutagenesis (Fig. 2). Residues R68, A71, R76, and S78 were selected because they appear to interact with the 2′ phosphate group of the bound NADPH. Q110 was selected for its potential to affect the cofactor orientation through interaction with the adenine moiety.

We generated and screened five individual libraries made by site-saturation mutagenesis at each position for NADPH and NADH depletion in the presence of 2-AL. Variants were selected for characterization when they displayed improved activity with NADH, while also exhibiting a higher ratio of NADH to NADPH activities. From these libraries, we obtained ten variants with increased specific activities in the presence of NADH in the screen. Table 1 summarizes the specific activities and kinetic parameters of representative variants (for complete specific activity data see Table C, Appendix A). Mutations at residues R68 (L), A71 (S, T), R76 (G, S), and Q110 (A, V) increased activity with NADH, resulting in NADH/NADPH activity ratios between 0.22 and 0.47 (wild-type ratio = 0.08). The aforementioned mutations also increased NADPH-dependent activity, albeit to a lesser degree. Mutation Q110V, for example, decreased the K_M for NADH and NADPH 8- and 3-fold, respectively, and increased k_{cat} values for both cofactors. The Q110V mutation thus improved the catalytic efficiencies for both cofactors, but retained higher activity with NADPH. We found three mutations, R76T, R76D, and S78D, that selectively increased activity in the presence of NADH, and S78D actually resulted in a switch in cofactor preference to NADH. Mutation S78D decreased the K_M for NADH 8-fold, while increasing the K_M

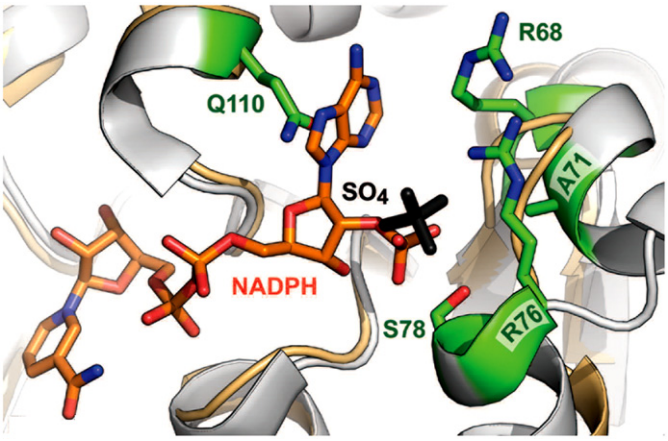

Fig. 2. Structural alignment of the NADPH-binding pocket of *E. coli* IlvC (PDB code 1yrl (Tyagi et al., 2005), white) with spinach KARI (PDB code 1yve (Biou et al., 1997), yellow). *E. coli* IlvC binds SO_4 (sticks, black), while spinach KARI binds NADPH (sticks, orange). *E. coli* site-saturation mutagenesis targets (sticks, green) are labeled. (For interpretation of the references to color in this figure legend, the reader is referred to the web version of this article.)

Table 1
Kinetic parameters of IlvC variants determined using NADPH or NADH, with 2-AL as substrate in excess.

Variant	Mutations	U/mg[a]		K_M [μM][b]		k_{cat} [s^{-1}]		k_{cat}/K_M [$M^{-1}s^{-1}$]		Ratio k_{cat}/K_M
		NADH	NADPH	NADH	NADPH	NADH	NADPH	NADH	NADPH	NADH/NADPH
$IlvC^{his6}$	–	0.08	1.00	1080	40	0.3	3.6	300	87,300	0.003
$IlvC^{A71S\text{-}his6}$	A71S	0.57	2.65	n.d.[c]	n.d.	n.d.	n.d.	n.d.	n.d.	n.d.
$IlvC^{R76D\text{-}his6}$	R76D	0.26	0.69	n.d.	n.d.	n.d.	n.d.	n.d.	n.d.	n.d.
$IlvC^{S78D\text{-}his6}$	S78D	1.00	0.61	130	660	3.6	2.5	27,600	3,800	7.0
$IlvC^{Q110V\text{-}his6}$	Q110V	0.93	2.00	140	13	3.3	7.2	24,800	569,000	0.04
$IlvC^{Q110A\text{-}his6}$	Q110A	0.85	2.00	280	24	3.1	7.2	11,000	302,000	0.04
$IlvC^{B8\text{-}his6}$	S78D, Q110V	0.57	0.62	65	65	2.0	2.2	31,800	34,200	0.9
$IlvC^{6E6\text{-}his6}$	A71S, R76D, S78D, Q110V	0.65	0.07	30	650	2.3	0.2	74,000	400	185
$IlvC^{2H10\text{-}his6}$	A71S, R76D, S78D, Q110A	0.74	0.17	40	570	2.6	0.6	60,300	1100	55

All enzymes were purified prior to characterization. The mutations are given relative to wild-type IlvC. Each value represents the average of three independent measurements. The resulting standard errors were within 5%.

[a] The enzyme activities were determined in 250 mM potassium phosphate pH 7 with 1 mM DTT, 200 μM NADPH or NADH, 10 mM 2-AL, and 10 mM $MgCl_2$. The concentrations of the purified enzymes were determined using Bradford assay.

[b] The Michaelis–Menten constants for cofactors were measured with appropriate dilutions of NADPH and NADH in the presence of saturating concentrations of substrate 2-AL (10 mM).

[c] n.d.—Not determined.

for NADPH 16-fold. In addition, the k_{cat} of the S78D variant for NADH increased to match the wild-type k_{cat} for NADPH. However, the catalytic efficiency of IlvC$^{S78D\text{-}his6}$ using NADH was still only 32% of wild-type catalytic efficiency on NADPH, with a selectivity of 7:1 for NADH. We then added the best generally activating mutation, Q110V, to IlvC$^{S78D\text{-}his6}$. The resulting double mutant unfortunately lost S78D's NADH preference.

A library was constructed in which all beneficial mutations as well as the wild-type residues were recombined. The resulting library was screened to full coverage (all variants sampled with 95% confidence) for cofactor depletion in the presence of 2-AL. We rescreened 26 variants, of which eight were expressed and purified. Six of the eight variants showed specific activities ranging from 0.44–0.55 U/mg with NADH, but also had retained or even improved specific activities with NADPH (0.72–2.62 U/mg). Only two IlvC variants, IlvC$^{2H10\text{-}his6}$ (A71S:R76D:S78D:Q110A) and IlvC$^{6E6\text{-}his6}$ (A71S:R76D:S78D:Q110V), were found to have higher 2-AL specific activity with NADH than with NADPH (0.74 vs. 0.17 U/mg and 0.65 vs. 0.07 U/mg). The K_M values of these variants for NADH, 40 and 30 μM, rivaled the wild-type K_M for NADPH of 40 μM. The catalytic efficiencies of IlvC$^{2H10\text{-}his6}$ and IlvC$^{6E6\text{-}his6}$ on NADH, 60,300 and 74,000 $M^{-1}s^{-1}$, were 70% and 85% of wild-type catalytic efficiency with NADPH, respectively. The best variant, IlvC$^{6E6\text{-}his6}$, exhibited a specificity of 185:1 for NADH, which corresponds to a 54,000-fold change.

3.2. Engineering of L. lactis AdhA

In the NADPH-dependent pathway (Atsumi et al., 2008b), the native NADPH-dependent *E. coli* ADH, YqhD, reduces isobutyraldehyde to isobutanol. Atsumi and coworkers identified the NADH-dependent *L. lactis* AdhA as compatible with the pathway (Atsumi et al., 2010). Whereas substituting YqhD with wild-type AdhA resulted in comparable titers under micro-aerobic conditions (Atsumi et al., 2010), the *in vitro* K_M of AdhA (11.7 mM) for isobutyraldehyde was 10-fold higher than that of YqhD (1.8 mM). We hypothesized that the AdhA K_M for isobutyraldehyde could be decreased and that a variant with higher catalytic efficiency should generate higher isobutanol titers. From screening approximately 4000 clones of a random mutagenesis library for increased isobutyraldehyde reduction activities in cell-free extracts, we identified two variants with at least 3-fold decreased K_M values. Recombination of the mutations from variants AdhA$^{28E7\text{-}his6}$ (N219Y and L264V) and AdhA$^{30C11\text{-}his6}$ (Y50F and I212T) yielded variant AdhA$^{RE1\text{-}his6}$ with mutations Y50F, I212T, and L264V and a K_M for isobutyraldehyde similar to that of YqhD (Table 2). Furthermore, the k_{cat} increased 4-fold and the catalytic efficiency 40-fold for isobutyraldehyde with respect to wild-type AdhA.

Table 2
Kinetic parameters of AdhA variants measured with isobutyraldehyde in the presence of NADH as cofactor.

Variant	Mutations	K_M [mM]	k_{cat} [s^{-1}]	k_{cat}/K_M [$M^{-1}s^{-1}$]
AdhA^{his6}	-	11.7	30	2800
AdhA$^{28E7\text{-}his6}$	N219Y, L264V	2.7	60	21,000
AdhA$^{30C11\text{-}his6}$	Y50F, I212T	3.9	80	20,000
AdhA$^{RE1\text{-}his6}$	Y50F, I212T, L264V	1.7	140	82,000

All enzymes were purified prior to characterization. The mutations are given relative to wild-type AdhA. Each value represents the average of three independent measurements. The resulting standard errors were within 5%.
The enzyme assays were conducted in 100 mM Tris–HCl pH 7 with 1 mM DTT, 200 μM NADH, and 10 mM isobutyraldehyde. The concentrations of the purified enzymes were determined using the Bradford assay. The Michaelis–Menten constants for the substrate were measured with appropriate dilution series of isobutyraldehyde.

3.3. Anaerobic NADH-dependent fermentations in E. coli

Using the NADH-dependent IlvC$^{6E6\text{-}his6}$ variant (Table 1) in conjunction with wild-type AdhA and AdhA^{RE1}, we were able to construct NADH-dependent isobutanol fermentation pathways that consumed the NADH produced during glycolysis (Fig. 1). The three additional enzymes of the isobutanol pathway, acetolactate synthase, dihydroxy-acid dehydratase, and 2-keto-acid decarboxylase, were integrated into the genome of production strain 1993. Six plasmids, pGVferm1–6 encoding the different ADH and IlvC combinations IlvC^{his6}/YqhD, IlvC^{his6}/AdhA, IlvC^{his6}/AdhA^{RE1}, IlvC$^{6E6\text{-}his6}$/YqhD, IlvC$^{6E6\text{-}his6}$/AdhA, and IlvC$^{6E6\text{-}his6}$/AdhA^{RE1}, were used to complement the partial pathway. These combinations created solely NADPH-dependent, solely NADH-dependent, and mixed-cofactor dependent pathways. A knock-in of the PntAB transhydrogenase under the control of the P_LLacO_1 promoter (Lutz and Bujard, 1997) into the *sthA* locus of 1993 was also prepared, so that we could compare the NADH–NADPH interconversion approach to that of balancing cofactor utilization.

As illustrated in Fig. 3A, the NADPH-dependent pathway produced an isobutanol titer of only 1 g/L after 24 h under anaerobic conditions. Exchanging one of the two NADPH-dependent enzymes with an NADH-dependent homolog improved the titer 2- (IlvC/AdhA) to 3-fold (IlvC$^{6E6\text{-}his6}$/YqhD). Using either the transhydrogenase-expressing strain or the NADH-dependent pathway containing IlvC$^{6E6\text{-}his6}$ and AdhA increased the titer 8.5-fold over the NADPH-dependent pathway. The highest isobutanol titer, 13.4 g/L, was achieved with the NADH-dependent enzyme combination IlvC$^{6E6\text{-}his6}$ and AdhA^{RE1}. Specific productivities increased significantly (38–88%) when only one of the NADPH-dependent enzymes was replaced (Fig. 3B). Despite having similar isobutanol titers, the PntAB-expressing strain showed a higher specific productivity than the IlvC$^{6E6\text{-}his6}$/AdhA expressing strain, 0.082 g/L/h/OD vs. 0.068 g/L/h/OD, due to either lower cell mass produced by the PntAB-expressing strain or differences in activity between YqhD and AdhA employed in the strains. Finally, utilizing AdhA^{RE1} in conjunction with IlvC$^{6E6\text{-}his6}$ improved specific productivity 6-fold over the NADPH-dependent pathway, enabling this strain to surpass the productivity of the transhydrogenase-expressing strain. Improvements in the anaerobic yield (for calculation see Table D, Appendix A) can be obtained by replacing one of the two NADPH-dependent enzymes (Fig. 3C): the NADPH-dependent pathway reached an anaerobic yield of only 53%, whereas strains expressing either an NADH-dependent IlvC or ADH produced isobutanol at 74 to 82% yield. The yield for the fully NADH-dependent AdhA^{RE1}/IlvC$^{6E6\text{-}his6}$ pathway increased even more, reaching 100% of the theoretical, rivaling the result of the PntAB containing strain, expressing the NADPH-dependent pathway.

4. Discussion

Conversion of glucose to pyruvate via glycolysis in *E. coli* leads to the production of two equivalents of NADH. The isobutanol biosynthetic pathway introduced in *E. coli* by Liao and coworkers (Atsumi et al., 2008b) consumes two NADPH for each pyruvate converted to isobutanol, leading to a cofactor imbalance in the cell. Under aerobic conditions, the cell can provide NADPH for isobutanol production through the tricarboxylic acid (TCA) cycle or the pentose phosphate pathway (PPP), and the theoretical isobutanol yield per glucose is only 0.86 (mole/mole) (for calculation see Table E, Appendix A). Since feedstock cost is the major component of the overall production cost, increases in yield directly improve the economic viability of isobutanol production (Stephanopoulos, 2007). Thus, the TCA cycle and PPP should be

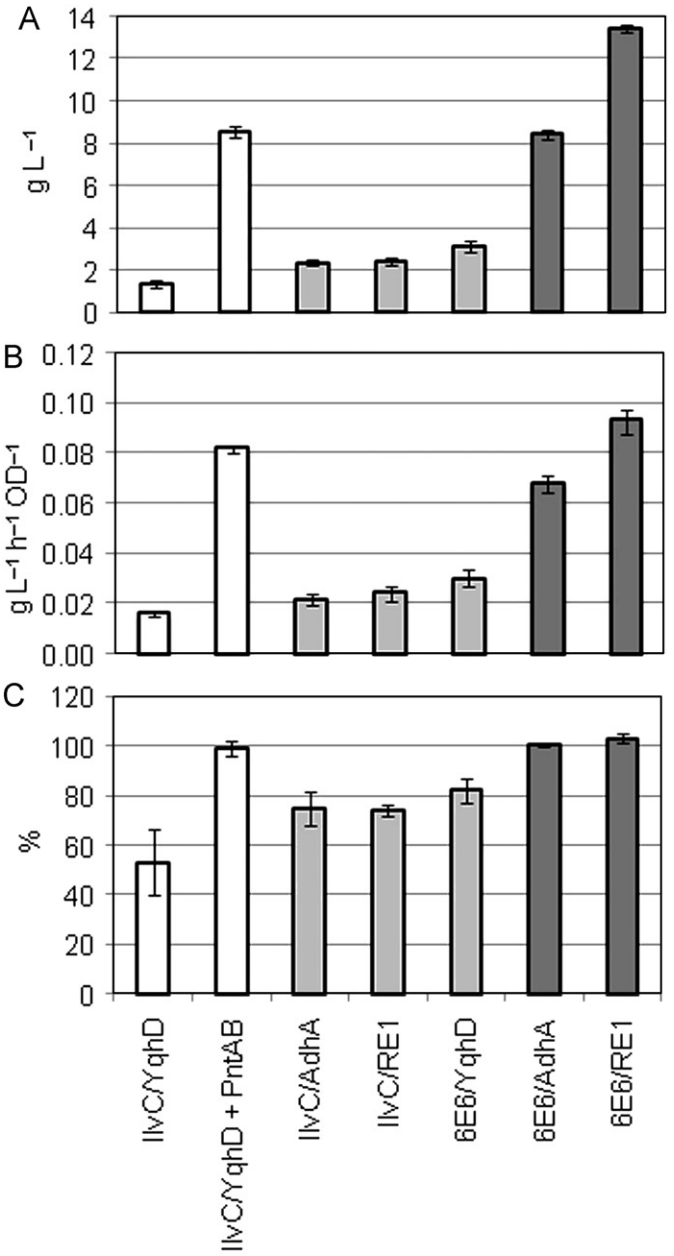

Fig. 3. (A) Anaerobic isobutanol titer [g/L]; (B) specific productivity [g/L/h/OD]; and (C) anaerobic theoretical yield [%] (for calculation see Table D, Appendix A). A, B, and C were determined after 24 h. Cells were grown aerobically at 37 °C in M9 salts (Miller, 1992) supplemented with 8.5% glucose, 10 g/L yeast extract, 10 μM ferric citrate, 2 mM $MgSO_4$, 0.1 mM $CaCl_2$, and trace metals, until they reached an OD_{600} of 0.8–1.0. After induction, cultures continued to grow at 30 °C until an OD_{600} of 4–6 was reached. Cells were then shifted to anaerobic conditions. The strains were kept under strictly anaerobic conditions for the duration of the fermentation. The error bars are based on biological triplicates. White columns: NAD**P**H/NAD**P**H-dependent pathways; light gray columns: NAD**P**H/NADH-dependent pathways; and dark gray columns: NADH/NADH-dependent pathways.

avoided to maximize the yield. We hypothesized that resolving the cofactor imbalance would enable anaerobic isobutanol fermentation approaching the theoretical maximum yield of one isobutanol produced per glucose consumed.

Exploring this hypothesis, we implemented two different approaches to resolving the cofactor imbalance. Use of PntAB has been described to regenerate NADPH in the production of chiral alcohols from ketones using whole cells (Weckbecker and Hummel, 2004) or to increase production of chemicals that rely on NADPH-dependent biosynthetic pathways (Kabus et al., 2007). Although over-expression of a transhydrogenase is an easy solution to balance cofactor utilization in an engineered metabolic pathway in *E. coli*, the result of direct implementation in yeast or other industrial microorganisms will be unpredictable, since the transhydrogenase may not always shift the hydride ion in the correct direction (Nissen et al., 2001). Changing the cofactor specificity of the pathway enzymes to match the available reducing equivalents would be a more general solution. Such an approach has improved ethanol yields of xylose fermentations having an overall cofactor imbalance due to differences in the cofactor preferences of the xylose reductase and xylose dehydrogenase (Bengtsson et al., 2009; Jeppsson et al., 2006).

A common strategy for engineering enzyme cofactor specificity in the absence of structural information is to substitute either aspartic or glutamic acid for highly conserved, positively charged residues in the NADPH-binding site (Scrutton et al., 1990) with the goal of disrupting the salt bridge to the NADPH 2′ phosphate group. Introducing a negatively charged side chain generally lowers NADPH affinity and is sometimes sufficient to switch the cofactor specificity in favor of NADH. However, this improved specificity for NADH is often accompanied by loss of activity (Clermont et al., 1993; Rane and Calvo, 1997; Scrutton et al., 1990). Rane and Calvo pursued this approach with *E. coli* IlvC, targeting four positively charged residues (R68, K69, K75, and R76) for mutagenesis. Although their variant, R68D:K69L:K75V:R76D, exhibited a change in cofactor preference (Rane and Calvo, 1997), it was unable to support anaerobic isobutanol fermentation. Engineering an enzyme whose catalytic efficiency with its new cofactor is comparable to that of the native enzyme with its native cofactor requires more intricate remodeling of the cofactor-binding site, which is enabled by an accumulated wealth of structural information (Khoury et al., 2009) and methods of directed enzyme evolution (Romero and Arnold, 2009).

We performed saturation mutagenesis at five amino acid residues in the Rossmann fold of the IlvC cofactor-binding site. These residues are highly conserved in known KARI sequences, all of which are NADPH-dependent. Mutations that increased NADH activity were identified at all five positions. Unexpectedly, several of these mutations also improved the native NADPH-dependent specific activity. Of the mutations that improved specific NADH activity, a rationale can be offered for R76D, whose guanidinium group appears to be in position to form a salt bridge with the 2′ phosphate of NADPH (Tyagi et al., 2005). A mutation at position 76 would disrupt the native salt bridge, while introducing a negative charge would disfavor NADPH binding. Mutation R76D, in fact, leads to the loss of NADPH activity. Its slight improvement in NADH activity is insufficient to switch the activity ratio in favor of NADH, which suggests that other residues within the binding pocket contribute to NADPH binding. The only single mutation that switched cofactor preference from NADPH to NADH was S78D, which also introduces a negative charge in the binding pocket. In addition to disfavoring NADPH binding through steric and electrostatic interactions with the 2′ phosphate group, S78D could induce a new salt-bridge conformation for nearby R76, thereby reducing the latter's contribution to NADPH binding. Although S78D switched the cofactor preference in favor of NADH, no single mutant replicated the catalytic efficiency of native IlvC utilizing NADPH. Subsequent recombination of beneficial mutations, however, allowed us to identify two quadruple mutants with 70–85% of the parental enzyme's catalytic efficiency. These two variants, $IlvC^{6E6\text{-}his6}$ and $IlvC^{2H10\text{-}his6}$, contained the best mutations at A71, R76, and S78 and differed only at position Q110. Of the four mutations, only R76D is shared with the variant identified by Rane and Calvo (1997).

Based on the excellent *in vitro* catalytic properties of $IlvC^{6E6\text{-}his6}$, we expected it to effectively substitute for its

wild-type counterpart in the isobutanol pathway. We combined IlvC$^{6E6\text{-}his6}$ with wild-type AdhA and also with the engineered variant AdhA^{RE1} in the isobutanol pathway to study the performance of these NADH-dependent pathways under anaerobic conditions. In addition, AdhA and each of the engineered enzymes, AdhA^{RE1} and IlvC$^{6E6\text{-}his6}$, were investigated individually for their ability to support anaerobic isobutanol production. Cells expressing the NADPH-utilizing pathway have little means to counteract the cofactor imbalance during the anaerobic phase of isobutanol production; essentially, production is supported by NADPH already present in the cells when anaerobic fermentation starts and by the limited activity of the native PntAB, and possibly by *SthA* (Sanchez et al., 2006). The low yield and low isobutanol titer of the NADPH-dependent pathway under anaerobic conditions indicate that the endogenous transhydrogenases are unable to maintain the NADPH flux needed for the complete conversion of glucose to isobutanol. In fact, when the endogenous transhydrogenase activity is augmented by the integration of an inducible copy of the *pntAB* gene, isobutanol is produced at the theoretical yield. Exchanging just one of the two NADPH-dependent enzymes did not enable the pathway to reach the theoretical yield. However, by reducing half of the NADPH demand from an isobutanol production, the titer was doubled, as was the specific productivity, and higher yields were achieved. Replacement of both NADPH-utilizing enzymes with the engineered NADH-dependent variants achieved 100% yield. The true advantage of the cofactor-balanced pathway over the transhydrogenase approach, however, emerges in the 1.7-fold higher isobutanol titer. This difference can be attributed to relieving the metabolic strain of proton translocation catalyzed by PntAB. The anaerobic titers presented in this study equal (PntAB strain and IlvC$^{6E6\text{-}his6}$/AdhA) and exceed (IlvC$^{6E6\text{-}his6}$/AdhA^{RE1}) by a remarkable 1.6-fold of the isobutanol titer previously reported under micro-aerobic conditions after 24 h (Atsumi et al., 2010). The notable differences observed among the NADH-dependent AdhA and AdhA^{RE1} strains' specific productivities and titers could reflect the different K_M values of the ADHs for isobutyraldehyde.

By completely removing the pathway's dependence on NADPH, we overcame an essential obstacle to anaerobic fermentation with an engineered isobutanol pathway and obtained isobutanol titers at 100% theoretical yield. While over-expression of PntAB was also able to resolve the cofactor imbalance and achieve 100% theoretical yield, the titer and productivity of this strain lagged behind the strain utilizing fully competent NADH-utilizing enzymes. Resolving cofactor imbalances using engineered enzymes is an approach applicable to other production microorganisms and biofuel pathways, and should enable the production of desirable higher-alcohol fuels with industrially relevant titers under anaerobic conditions.

Acknowledgments

Research was sponsored by the U.S. Army Research Laboratory and was accomplished under cooperative Agreement no. W911NF-09-2-0022. The views and conclusions contained in this document are those of the authors and should not be interpreted as representing the official policies, either expressed or implied, of the Army Research Laboratory or the U.S. Government. The U.S. Government is authorized to reproduce and distribute reprints for Government purposes notwithstanding any copyright notation herein. J.T.M. is supported by the Department of Defense through the National Defense Science & Engineering Graduate Fellowship Program and by the National Science Foundation through the Graduate Research Fellowship Program. X.L. is supported by the China Scholarship Council (CSC).

Appendix A. Supplementary materials

Supplementary data associated with this article can be found in the online version at doi:10.1016/j.ymben.2011.02.004.

References

Alper, H., Stephanopoulos, G., 2009. Engineering for biofuels: exploiting innate microbial capacity or importing biosynthetic potential? Nat. Rev. Microbiol. 7, 715–723.

Atsumi, S., Cann, A.F., Connor, M.R., Shen, C.R., Smith, K.M., Brynildsen, M.P., Chou, K.J.Y., Hanai, T., Liao, J.C., 2008a. Metabolic engineering of *Escherichia coli* for 1-butanol production. Metab. Eng. 10, 305–311.

Atsumi, S., Hanai, T., Liao, J.C., 2008b. Non-fermentative pathways for synthesis of branched-chain higher alcohols as biofuels. Nature 451, 86–89.

Atsumi, S., Wu, T.Y., Eckl, E.M., Hawkins, S.D., Buelter, T., Liao, J.C., 2010. Engineering the isobutanol biosynthetic pathway in *Escherichia coli* by comparison of three aldehyde reductase/alcohol dehydrogenase genes. Appl. Microbiol. Biotechnol. 85, 651–657.

Bengtsson, O., Hahn-Hagerdal, B., Gorwa-Grauslund, M.F., 2009. Xylose reductase from *Pichia stipitis* with altered coenzyme preference improves ethanolic xylose fermentation by recombinant *Saccharomyces cerevisiae*. Biotechnol. Biofuels (2).

Biou, V., Dumas, R., CohenAddad, C., Douce, R., Job, D., PebayPeyroula, E., 1997. The crystal structure of plant acetohydroxy acid isomeroreductase complexed with NADPH, two magnesium ions and a herbicidal transition state analog determined at 1.65 angstrom resolution. EMBO J. 16, 3405–3415.

Bloom, J.D., Labthavikul, S.T., Otey, C.R., Arnold, F.H., 2006. Protein stability promotes evolvability. In: Proc. Natl. Acad. Sci. USA 103, 5869–5874.

Bruno, T.J., Wolk, A., Naydich, A., 2010. Composition-explicit distillation curves for mixtures of gasoline and diesel fuel with gamma-valerolactone. Energy Fuels 24, 2758–2767.

Chao, G., Lau, W.L., Hackel, B.J., Sazinsky, S.L., Lippow, S.M., Wittrup, K.D., 2006. Isolating and engineering human antibodies using yeast surface display. Nat. Protocols 1, 755–768.

Chin, J.W., Khankal, R., Monroe, C.A., Maranas, C.D., Cirino, P.C., 2009. Analysis of NADPH supply during xylitol production by engineered *Escherichia coli*. Biotechnol. Bioeng. 102, 209–220.

Chunduru, S.K., Mrachko, G.T., Calvo, K.C., 1989. Mechanism of ketol acid reductoisomerase—steady-state analysis and metal-ion requirement. Biochemistry-US. 28, 486–493.

Clarke, D.M., Bragg, P.D., 1985. Cloning and expression of the transhydrogenase gene of *Escherichia coli*. J. Bacteriol. 162, 367–373.

Clermont, S., Corbier, C., Mely, Y., Gerard, D., Wonacott, A., Branlant, G., 1993. Determinants of coenzyme specificity in glyceraldehyde-3-phosphate dehydrogenase—role of the acidic residue in the fingerprint region of the nucleotide-binding fold. Biochemistry-US. 32, 10178–10184.

Connor, M.R., Liao, J.C., 2009. Microbial production of advanced transportation fuels in non-natural hosts. Curr. Opinion Biotechnol. 20, 307–315.

Datsenko, K.A., Wanner, B.L., 2000. One-step inactivation of chromosomal genes in *Escherichia coli* K-12 using PCR products. In: Proc. Natl. Acad. Sci. USA 97, 6640–6645.

Ehrlich, F., 1907. Concerning the conditions for fusel oil formation and concerning its connection with the protein formation in yeast. Ber. Dtsch. Chem. Ges. 40, 1027–1047.

Ehsani, M., Fernandez, M.R., Biosca, J.A., Dequin, S., 2009. Reversal of coenzyme specificity of 2,3-butanediol dehydrogenase from *Saccharomyces cerevisae* and *in vivo* functional analysis. Biotechnol. Bioeng. 104, 381–389.

Hazelwood, L.A., Daran, J.M., van Maris, A.J.A., Pronk, J.T., Dickinson, J.R., 2008. The Ehrlich pathway for fusel alcohol production: a century of research on *Saccharomyces cerevisiae* metabolism. Appl. Environ. Microbiol. 74, 2259–2266.

Horton, R.M., Hunt, H.D., Ho, S.N., Pullen, J.K., Pease, L.R., 1989. Engineering hybrid genes without the use of restriction enzymes—gene-splicing by overlap extension. Gene 77, 61–68.

Jeppsson, M., Bengtsson, O., Franke, K., Lee, H., Hahn-Hagerdal, R., Gorwa-Grauslund, M.F., 2006. The expression of a *Pichia stipitis* xylose reductase mutant with higher Km for NADPH increases ethanol production from xylose in recombinant *Saccharomyces cerevisiae*. Biotechnol. Bioeng. 93, 665–673.

Jornvall, H., Persson, B., Jeffery, J., 1987. Characteristics of alcohol polyol dehydrogenases—the zinc-containing long-chain alcohol dehydrogenases. Eur. J. Biochem. 167, 195–201.

Kabus, A., Georgi, T., Wendisch, V.F., Bott, M., 2007. Expression of the *Escherichia coli pntAB* genes encoding a membrane-bound transhydrogenase in *Corynebacterium glutamicum* improves L-lysine formation. Appl. Microbiol. Biotechnol. 75, 47–53.

Khoury, G.A., Fazelinia, H., Chin, J.W., Pantazes, R.J., Cirino, P.C., Maranas, C.D., 2009. Computational design of *Candida boidinii* xylose reductase for altered cofactor specificity. Protein Sci. 18, 2125–2138.

Krampitz, L.O., 1957. Preparation and determination of acetoin, diacetyl, and acetolacetate. Methods Enzymol. 3, 277–283.

Kunkel, T.A., Roberts, J.D., Zakour, R.A., 1987. Rapid and efficient site-specific mutagenesis without phenotypic selection. Methods Enzymol. 154, 367–382.

Liu, T., Khosla, C., 2010. Genetic engineering of *Escherichia coli* for biofuel production. Annu. Rev. Genet. 44, 53–69.

Lutz, R., Bujard, H., 1997. Independent and tight regulation of transcriptional units in *Escherichia coli* via the LacR/O, the TetR/O and AraC/I-1-I-2 regulatory elements. Nucleic Acids Res. 25, 1203–1210.

Matsushika, A., Watanabe, S., Kodaki, T., Makino, K., Inoue, H., Murakami, K., Takimura, O., Sawayama, S., 2008a. Expression of protein engineered NADP plus-dependent xylitol dehydrogenase increases ethanol production from xylose in recombinant *Saccharomyces cerevisiae*. Appl. Microbiol. Biotechnol. 81, 243–255.

Matsushika, A., Watanabe, S., Kodaki, T., Makino, K., Sawayama, S., 2008b. Bioethanol production from xylose by recombinant *Saccharomyces cerevisiae* expressing xylose reductase, NADP(+)-dependent xylitol dehydrogenase, and xylulokinase. J. Biosci. Bioeng. 105, 296–299.

Miller, J.H., 1992. A Short Course in Bacterial Genetics: A laboratory manual and handbook for *Escherichia coli* and related bacteria. Cold Spring Harbor Laboratory Press, Cold Spring Harbor, N.Y.

Nissen, T.L., Anderlund, M., Nielsen, J., Villadsen, J., Kielland-Brandt, M.C., 2001. Expression of a cytoplasmic transhydrogenase in *Saccharomyces cerevisiae* results in formation of 2-oxoglutarate due to depletion of the NADPH pool. Yeast 18, 19–32.

Petschacher, B., Nidetzky, B., 2008. Altering the coenzyme preference of xylose reductase to favor utilization of NADH enhances ethanol yield from xylose in a metabolically engineered strain of *Saccharomyces cerevisiae*. Microb. Cell Fact. (7).

Rane, M.J., Calvo, K.C., 1997. Reversal of the nucleotide specificity of ketol acid reductoisomerase by site-directed mutagenesis identifies the NADPH binding site. Arch. Biochem. Biophys. 338, 83–89.

Romero, P.A., Arnold, F.H., 2009. Exploring protein fitness landscapes by directed evolution. Nat. Rev. Mol. Cell Biol. 10, 866–876.

Rude, M.A., Schirmer, A., 2009. New microbial fuels: a biotech perspective. Curr. Opinion Microbiol. 12, 274–281.

Sambrook, J., Frisch, E.F., Maniatis, T., 1989. Molecular Cloning: A Laboratory Manual. Cold Spring Harbor Laboratory Press, New York.

Sanchez, A.M., Andrews, J., Hussein, I., Bennett, G.N., San, K.Y., 2006. Effect of overexpression of a soluble pyridine nucleotide transhydrogenase (UdhA) on the production of poly(3-hydroxybutyrate) in *Escherichia coli*. Biotechnol. Progress. 22, 420–425.

Sauer, U., Canonaco, F., Heri, S., Perrenoud, A., Fischer, E., 2004. The soluble and membrane-bound transhydrogenases UdhA and PntAB have divergent functions in NADPH metabolism of *Escherichia coli*. J. Biol. Chem. 279, 6613–6619.

Scrutton, N.S., Berry, A., Perham, R.N., 1990. Redesign of the coenzyme specificity of a dehydrogenase by protein engineering. Nature 343, 38–43.

Shen, C.R., Liao, J.C., 2008. Metabolic engineering of *Escherichia coli* for 1-butanol and 1-propanol production via the keto-acid pathways. Metab. Eng. 10, 312–320.

Steen, E.J., Chan, R., Prasad, N., Myers, S., Petzold, C.J., Redding, A., Ouellet, M., Keasling, J.D., 2008. Metabolic engineering of *Saccharomyces cerevisiae* for the production of n-butanol. Microb. Cell Fact., 7.

Stephanopoulos, G., 2007. Challenges in engineering microbes for biofuels production. Science 315, 801–804.

Szwaja, S., Naber, J.D., 2010. Combustion of n-butanol in a spark-ignition IC engine. Fuel 89, 1573–1582.

Taylor, J.D., Jenni, M.M., Peters, M.W., 2010. Dehydration of fermented isobutanol for the production of renewable chemicals and fuels. Top. Catal. 53, 1224–1230.

Tyagi, R., Duquerroy, S., Navaza, J., Guddat, L.W., Duggleby, R.G., 2005. The crystal structure of a bacterial Class II ketol-acid reductolsomerase: domain conservation and evolution. Protein Sci. 14, 3089–3100.

Weckbecker, A., Hummel, W., 2004. Improved synthesis of chiral alcohols with *Escherichia coli* cells co-expressing pyridine nucleotide transhydrogenase, NADP(+)-dependent alcohol dehydrogenase and NAD(+)-dependent formate dehydrogenase. Biotechnol. Lett. 26, 1739–1744.

Yan, Y., Liao, J., 2009. Engineering metabolic systems for production of advanced fuels. J. Ind. Microbiol. Biot. 36, 471–479.